ABSTRACT

Monthly ERBE and CERES measurements are used to study the response of cloud radiative forcing to changes in sea surface temperature during the two El niño events of 1987 and 1998. We show that the response of cloud forcing to SST over the whole tropics is very different from that to local SST changes. In both El niño events, longwave cloud radiative forcing in the whole tropics decreases with SST, permitting more radiation escaping the Earth-atmosphere system, a negative contribution to the overall cloud feedback. The shortwave cloud radiative forcing in the whole tropics increases with SST, corresponding to less reflection of shortwave radiation to space, a positive contribution to the cloud feedback. These diagnostics are used as a means to understand the large-scale cloud processes rather than to infer the sign of cloud feedback. It is emphasized that the cloud variation in the 1987 El niño event is asscoated with a displacement of the warm pool and the Walker circulation, while that in 1998 is associated with the collapse of the Walker circulation.

1. Introduction

Clouds as one of the moist fluid dynamical phenomena play a subtle role in the Earth's climate. Clouds act as a greenhouse ingredient to warm the Earth. Clouds also reflect solar radiation to the space to cool the Earth. The net radiative effect of these two competing processes depends the height, type, and the optical properties of the clouds. All these characteristics vary in a climate change. Clouds thus exert a feedback to any forced climate change. This cloud-climate feedback problem was first studied by Schneider (1972) and Cess (1975). Later, it was found by Cess et al. (1989) that difference in cloud-climate feedback contributes to a three-fold difference in the sensitivity of a large group of general circulation models (GCMs). At the same time, Mitchell et al. (1989) showed that different treatments of clouds in the GCMs can lead to either amplification or damping of the global warming scenario in response to the increasing level of carbon dioxide in the atmosphere. These studies stimulated many subsequent research on this topic and they initiated national programs such as the Atmospheric Radiation Measurement Program (ARM) of the Department of Energy.

Cloud radiative forcing (CRF), first introduced in Charlock and Ramanathan (1985), can be conveniently used to quantify the radiative impact of clouds. It is defined as the influence of clouds on the input of radiant energy to the Earth-atmosphere system at the top-of-the-atmosphere (TOA). If we use F to denote the outgoing longwave radiation at TOA, and Q to denote the net downward shortwave radiation at TOA, and if we use subscript c to denote clear-sky quantities, the longwave (LW) CRF is defined as:

$$\text{LW CRF} = F_c - F \quad (1)$$

It is typically positive, describing the trapping of longwave by clouds (Ramanathan et al. 1989). The shortwave (SW) CRF is defined as

$$\text{SW CRF} = Q - Q_c \quad (2)$$

It is typically negative, describing the reduction of solar energy due to cloud reflections. The net CRF, or the total CRF, is simply the sum of the two.

The feedback of clouds on the climate system can then be defined as the variation of CRFs in a climate change. In a global warming scenario, if the change of cloud radiative forcing is positive, variation of clouds acts to trap more radiant energy in the climate system and thus it amplifies the climate warming, a positive feedback. If the change is negative, clouds act to mediate the climate change by disposing more radiant energy to space.

Cess and Potter (1988) designed an elegant method of understanding cloud feedback mechanisms in GCMs. They imposed a change in the sea-surface temperature in the models to diagnose the response of cloud radiative forcing at the TOA. The present paper follows Cess and Potter (1988) with the attempt to study the process of cloud forcing changes by using observational data. The Earth Radiation Budget Experiments (ERBE) measurements, and the Clouds and the Earth's Radiant Energy System (CERES) measurements, which provided the timely needed cloud-radiative forcing data, span the two El niño events of 1987 and 1998. These two El niño events are used as case studies to learn how cloud forcing responds to SST changes. Our interest is in

the energy budget of the Earth-Atmosphere system rather than in the local responses. Zhang et al. (1996) has reported the relationship between variations of cloud forcing and sea surface temperatures (SSTs) in the 1987 El niño event using five years of ERBE data from January 1985 to December 1989. The present paper extends this analysis to include the CERES measurements. It also differs from Zhang et al. (1996) in that only ERBS measurements are used in order to minimize differences caused by the different satellite sampling methods.

The purpose of the paper is not to answer whether cloud feedback is positive or negative in a global climate change. Instead, it is to show how cloud feedback is affected by the compensating geographical distribution of cloud changes in a large domain. We show from the analysis of the two El niño events that warm tropics is associated with reduced longwave greenhouse effect of clouds, and less reflection of solar radiation to space, which is in sharp contrast to the SST relationship in the Eastern tropical pacific or in the western tropical warm pool. Furthermore, we will show that different mechanisms may have caused this relationship between SST and cloud forcing for the two El niño events.

2. Data and procedure

Cloud Forcing

The ERBE S-4G product, released from the NASA Langley Research Center, consists of measurements from three satellites: ERBS from November 1984 to December 1989, NOAA-9 from February 1985 to January 1987, and NOAA-10 from November 1986 to

May 1989. ERBS is a precessing orbit satellite that samples a complete local diurnal cycle in about 36 days, while NOAA 9 and NOAA 10 are near sun-synchronous satellites that sample fixed local hours (around 14:30 and 07:30 local mean solar time respectively). The gridded monthly cloud radiative forcing data in the S-4G product was derived from the instantaneous radiance measurements through several steps. One of them is the modeling of the diurnal cycle. Because of the difference in the diurnal sampling among the three satellites, potential differences among ERBS and NOAA9, NOAA10 can be interpreted as El niño signatures. We therefore restrict the analysis of ERBE data to ERBS measurements. The data include fluxes under both all-sky and clear-sky conditions at a 2.5° by 2.5° resolution. The implementation of ERBE, including the technique to separately measure all-sky and clear-sky fluxes, can be found in Barkstrom and Smith (1986), Ramanathan et al. (1989), and Harrison et al. (1990).

The CERES ES-4G dataset covers the eight month period from January 1998 to August 1998. An overview of the CERES instrument and data algorithm can be found in Wielicki et al. (1995). The CERES instrument was on board the Tropical Rainfall Measurement Mission (TRMM) satellite, which also uses a precessing orbit that samples the whole diurnal cycle in about a month. The CERES ERBE-like product was processed using the same procedure as that used for the ERBE products. Validation of the CERES measurements against ERBE is not straightforward, because the CERES period covers the strong 1997-1998 El niño event and thus the underlying meteorological conditions are different. Wong et al. (2001) used a radiation model to

calculate clear-sky longwave flux by using the operational analysis and found consistencies between the calculated fluxes and the ERBE and CERES measurements. The difference is reported to be less than 1 Wm^{-2} in the whole tropics. The comparison for cloudy skies cannot be easily made because of lack of cloud microphysical and optical information. Potential differences are possible that are caused by different instruments and samplings from ERBE and CERES. There are no known causes, however. In the present study, we will use measurements from these two experiments to analyze the response of cloud forcing to the two El niño events, bearing in mind these sources of potential uncertainties.

There are grid points where cloud radiative forcing data are missing in the ERBE and CERES products. These missing grids are potentially important in contributing to the area averages of the cloud forcings, because missing CRF can occur in heavily overcast conditions where clear-sky scenes cannot be defined. Cloud forcing data at these missing grid points are estimated by first filling the missing clear-sky fluxes with values at the nearest grid boxes, and then by calculating the CRFs at these gird boxes.

b. SST

The sea surface temperature data are taken from the monthly National Meteorological Center analysis which is derived from ship, buoy and satellite measurements. Detailed description of the SST data can be found in Reynolds (1988), Reynolds and Smith (1994, 1995) and Smith and Reynolds (1998).

Figure 1a shows the annual variation of SST averaged over the equatorial Eastern Pacific (EEP, 10°N-10°S, 180°W – 90°W) for the years when there are ERBE or CERES measurements. The 1987 El niño is seen to start from the summer of 1986 and dissipate in the spring of 1988. In contrast, the 1998 SST only covers the ending part of an El niño event. It is also seen from the figure the first eight months of 1985, 1986 and 1989 can be considered as normal conditions.

Figure 1b shows the corresponding annual variations of SST in the entire tropical oceans from 30°N-30°S. Two features are noted. First, the tropical oceans as a whole are warmer during an El niño year than that in normal years, by as large as 0.7 °C. Second, there is clearly a delay in the dissipation of the El niño warming of the entire tropics relative to that in the EEP. Temperature in the entire tropical oceans approached normal condition in July of 1988 during the first El niño event, and at the end of 1998 in the second event, both with several months of delay to the counterparts in the EEP.

The warming of the entire tropical oceans during an El niño event is contributed by warming of SST in the tropical Indian Ocean and in the tropical Atlantic. Figures 2a and 2b show the eight-month averaged SST anomalies (January to August) with respect to the normal years of 1985, 1986 and 1989 for the two El niño events. In each El niño event, accompanying SST rise in the equatorial eastern pacific, SST anomalies are positive over the wider areas of the Indian Ocean and the Atlantic. Their magnitudes are larger than those of the negative SST anomalies in the western pacific and in the

subtropical Pacific. The positive anomalies reached 1.0 ^{o}C in these areas in 1998. Figure 2c shows the SST anomalies in 1998 for the first four months from January to April. Comparing with Figure 2b, it is seen that SST anomalies in the EEP, especially near the dateline, retreated significantly in the later months. The anomalies in the Indian Ocean and in the Atlantic, however, remain very similar in the later four months.

This phenomenon of SST change in the broad oceans is consistent with Meehl (1987) and Godfrey (1994) who reported that SSTs in the Indian Ocean warm up in their composite El niño event with magnitude reaching 0.4 K. This is also consistent with Villwock and Latif (1994) who reported that SST variations in the central and eastern tropical Pacific are typically followed by SST anomalies of the same sign in the Indian Ocean. The reason for this warming is not clear. Hirst and Godfrey (1993) suggested that the open passage at the southern tip of the Indonesia makes warm ocean currents to cross the Indian ocean and warm the SSTs there during an El niño event. To the contrary, Villwock and Latif (1994) argued that the surface wind forced by SST anomalies in the equatorial Pacific is the primary cause of the SST warming in the Indian Ocean. SST anomaly may even be a result of the cloud variations.

Although the SST anomaly patterns in these two El niño events are qualitatively similar, the difference in their magnitudes corresponds to potentially important differences in the SST forcing to the atmospheric circulation and clouds. Figure 3 shows the SST distributions in the normal years and in the two El Niño years averaged from January to August. In 1987, the negative SST anomaly in the western Pacific and

the positive SST anomaly in the central to eastern Pacific actually reflect a shift of the warm pool toward the dateline. In 1998, however, the maximum warming in the eastern Pacific leads to a SST distribution that is much more uniform in the zonal direction in the Pacific. Basin wide, the zonal SST gradient along the Pacific equator is 2 ^{o}C in 1998 versus about 5 ^{o}C in a normal year. This decrease in the zonal SST gradient has significant consequences on the atmospheric Walker circulation and subsequently the associated cloud processes, as will be discussed later.

3. Results

We first show the relationships of cloud forcing and SST in the EEP. Figure 4 shows the LW CRF and SW CRF against the SST in the EEP. Each solid circle in the figure represents an eight-month average for a given year. Consistent with several early studies, warmer SSTs are found to be associated with larger LW CRF, and smaller SW CRF, and thus more clouds. The 1998 data point from using the eight-month CERES measurements shows a remarkable consistency. This indirectly suggests that the CERES data are comparable with the ERBE data.

There is a large cancellation between the longwave and shortwave components (Kiehl, 1994). Zhang et al. (1996) showed that with the 2.5^{o} x 2.5^{o} grid data in the EEP, the sign of the net cloud forcing variation with SST follows that of the shortwave This change in cloud forcing, however, became statisticaly insignificant as the size of the area increases up to the who tropical Pacific. In view of the small magnitude of the

natural climate change in these years and the data length, we use the longwave and shortwave components as a vehicle to understand the cloud process.

Figure 5a shows the corresponding relationship between the area-averaged LW CRF and the SST in the entire tropics. In contrast to the SST-CRF relationship for the EEP, the warmer oceans are associated with smaller LW CRF. This is true for both the 1987-1988 El niño event, and the 1998 event. It is seen that the tropical oceans as a whole is much wamer in 1998 than that in the normal years, and the LW CRF over the entire tropics is much smaller than those in the normal years. Figure 5b shows the relationship between SW CRF and SST. Warm SSTs correspond to less reflection of radiation by clouds, even though the data points are more scattered than those in Figure 5a.

To gain some insight about the cause of the change of LW CRF with SST, Figure 6a and 6b show the geographical distributions of the anomalies of the LW CRF for the two El niño events. It is common in both events that the LW CRF increased in the central to eastern tropical Pacific where the SST anomaly is the maximum. Over many regions in the tropics, however, LW CRF is decreased. This is in sharp contrast to the SST anomalies shown in Figures 2a and 2b, in which the anomalies of SST are positive over the majority of the tropics.

The mechanisms of the decrease of the LW CRF in these two El niño events are, however, somewhat different. Figure 7 shows the basic distribution of the LW CRF. In a normal year, a well defined convective center is located in the western tropical Pacific

over the maritime continents, extending southeast along the South Pacific Convergence Zone (SPCZ) and eastward along the Intertropical Convergence Zone (ITCZ) in the eastern Pacific north of the equator. In the 1987 El niño event, the convective center is displaced toward the dateline, in response to the shift of the 29 ^{o}C line of warm pool shown in Figure 3. The overall structure of the center and the two extensions in the SPCZ and ITCZ are still similar to those in a normal year. In 1998, however, one can hardly define a convection center in the Pacific. A narrow line of maximum convection spans the whole tropical Pacific, apparently associated with the small zonal SST gradient shown in Figure 3c.

We shall show that in a normal year, there is a well defined Walker circulation in the tropical Pacific, and this Walker circulation is displaced in 1987, but it has almost collapsed in 1998. Figure 8a shows a height-longitude cross section of the zonal wind averaged from 5^{o}S to 5^{o}N and from January to August in a normal year. The wind data are from the National Environmental Prediction Center/National Center for Atmospheric Research (NCEP/NCAR) reanalysis. It is seen that east of 140^{o}E in the tropical Pacific, there are well defined easterlies in the lower troposphere and westeries in the upper troposphere, while to the west, there is a circulation cell that is opposite in directions. The 140^{o}E longitude roughly corresponds to the center of the upward branch of the Walker circulation and thus the maximum LW CRF. In 1987, this structure of the Walker circulation is changed (Figure 8b). Not only the magnitude of the easterlies and the westerlies all decreased, but also there was a shift in the upward branch toward the dateline, as indicated by the zero zonal wind line in the lower troposphere. This is also

consistent with the displaced center in LW CRF in Figure 6b. Nevertheless, one can still see the existence of the Walker circulation cell in 1987.

This picture changed dramatically in 1998 (Figure 8c). It is seen that easterlies prevail throughout the whole troposphere in the tropical Pacific. There is no well defined Walker circulation cell. This is apparently related with the small zonal SST gradient in the Pacific.

We shall also argue that 1998 is characterized by a well defined zonally symmetric Hadley circulation. Because of the uncertainties in the vertical velocity in the reanalysis products, we use the surface sea level pressure (SSP) to illustrate the differences among the different years. Figure 9 shows the SSP distribution in the tropical Pacific in the normal years, in 1987, and in 1998. One can see that the subtropical highs in 1998 in both hemispheres are stronger and are wider in their longitudinal dimension than those in a normal year and in 1998.

These changes in the large-scale atmospheric circulation are apparently responsible to the change in the cloud forcing. Cess et al. (2001) showed that the ratio of the magnitudes of SW CRF and the LW CRF is much larger in 1998 than those in other years. They inferred a significant change of the cloud vertical structures in 1998, with more middle and lower clouds in this event. The present analysis of the significant change in atmospheric circulation is consistent with their findings.

4. Summary

We have shown that in the two El niño events of 1987 and 1998, during which the whole tropical oceans are warmer than normal condition, the LW CRF averaged over the whole tropics decreased, a negative contribution to the cloud feedback; while the SW CRF averaged over the whole tropics increased, a positive contribution to the cloud feedback. This relationship is shown to be in sharp contrast to local SST-CRF relationships inferred from the tropical eastern Pacific. We have also shown that the signs of the CRF anomalies in the 1987 event are the result of compensating changes caused by the displacement of the warm pool and the associated Walker circulation; while the signs of the CRF anomalies in 1998 are related with the collapse of the Walker circulation. This analysis points to the need to understand the spatial structures of a climate change in order to study the cloud-climate feedback problem, since cloud feedbacks in a global warming scenario with SST changed to a more spatially uniform distribution versus a scenario with larger spatial SST gradient are likely to be very different.

ACKNOWLEDGEMENT: This research is supported by the National Science Foundation under grant ATM9701950 and by the Department of Energy under grant DEFG0298ER62570 to the State University of New York at Stony Brook.

REFERENCES

Barkstrom, B. R., and G. L. Smith, 1986: The Erath Radiation Budget Experiment: science and implementation, *Rev. Geophys.*, **24**, 379-390.

Cess, R. D., 1975: Global climate change – investigation of atmospheric feedback mechanisms. Tellus 27, 193-198.

Cess, R. D., and G. L. Potter, 1988: Exploratory studies of cloud radiative forcing with a general circulation model. Tellus, 39A, 460-473.

Cess, R. D. , et al, 1989: Interpretation of cloud-climate feedback as produced by 14 atmospheric general circulation models. *Science, 245, 513-516.*

Cess, R. D., M. H. Zhang, B. A. Wielicki, D. F. Young, X. L. Zhou, and Y. Nikitenko, 2001: the influence of the 1998 El niño upon cloud radiative forcing over the Pacific warm pool. J. Climate, in press.

Charlock, T. P., and V. Ramanathan, 1985: The albedo field and cloud radiative forcing produced by a general circulation model with internally generated cloud optics. J. Atmos. Sci., 42, 1408-1429.

Godfrey, J. S., 1994: A literature review of SST anomalies in the Indian Ocean: their effects on the atmosphere and their causes. *Proceedings of the International Conference on Monsoon Variability and Prediction,* Trieste, Italy, May 1994, 524-529.

Harrison, E. F., P. Minnis, B. R. Barkstrom, V. Ramanathan, R. D. Cess, and G. G. Gibson, 1990: Seasonal variation of cloud radiative forcing derived from the Earth radiation Budget experiment. *J. Geophy. Res.*, **95**, 18,687-18,703.

Hirst, A. C., and J. S. Godfrey, 1993: The role of the Indonesia Throughflow in a global ocean GCM. *J. Phys. Oceano.*, **23**, 1057-1086.

Kiehl, J. T., 1994: On the observed near cancellation between longwave and shortwave

cloud forcing in tropical regions. *J. Climate,* **7**, 559-565.

Meehl, G. A., 1987: The annual cycle and interannual variability in the tropical Pacific and Indian Ocean regions. *Mon. Wea. Rev.*, **115**, 1057-1086.

Mitchell, J. F. B., et al., 1989: CO_2 and climate: A missing feedback? *Nature,* 341, 132-134,

Ramanathan, V., R. D. Cess, E. F. Harrison, P. Minnis, B. R. Barkstrom, E. Ahmad, and D. Hartmann, 1989: Cloud-radiative forcing and climate: results from the Earth Radiation Budget Experiment. *Science*, **243**, 57-63.

Reynolds, R. W., 1988: A real-time global sea surface temperature analysis. *J. Climate*, **1**, 75-86.

Reynolds, R. W., and T. M. Smith, 1994: Improved global sea surface temperature analysis using optimum interpolation. J. Climate, 7, 929-948.

Reynolds, R. W., and T. M. Smith, 1995: A high-resolution global sea surface temperature climatology. J. Climate, 8, 1571-1583.

Schneidar, S. H., 1972: Cloudiness as a global climate feedback mechanism: the effects on radiation balance and surface temperature of variations in cloudiness. J. Atmos. Sci., 29, 1413-1422.

Smith, T. M., R. W. Reynolds, 1998: A high resolution global sea surface temperature climatology for the 1961-90 base period. J. Climate, 11, 3320-3323.

Villwock, A., and M. Latif, 1994: Indian Ocean response to ENSO. *Proceedings of the International Conference on Monsoon Variability and Prediction,* Trieste, Italy, May 1994, 530-537.

Wielicki, B. A., et al., 1995: Mission to Planet Earth: role of clouds and radiation in climate. Bull. Amer. Meteor. Soc., 76, 2215-2154.

Wong, T. D., D. F., Young, M. Haefflin, and S. Weckmann, 2001: On the validation of the CERES/TRMM ERBE-like monthly mean clear-sky dataset and the effects of the 1998 ENSO event. J. Climate, in press.

Zhang,, M. H., S. C. Xie, and R. D. Cess, 1996: Relationship between cloud-radiative-forcing and sea surface temperature over the entire tropical oceans. J. Climate, 9, 1374-1384.

FIGURE CAPTIONS

FIG. 1. Sea Surface Temperatures (SSTs) averaged over the eastern equatorial Pacific (a) and over the entire tropics (b).

FIG. 2. SST Anomalies (^{o}C) relative to the normal year of 1985, 1986 and 1989. (a) January to August, 1987. (b) January to August, 1998. (c) January to April, 1998.

FIG. 3. Distributions of SST (^{o}C) averaged from January to August. (a) Mean of 1985, 1986 and 1989. (b) 1987. (c) 1998.

FIG. 4. Relationship between cloud radiative forcings and SST in the eastern equatorial Pacific. (a) LW CRF versus SST. (b) SW CRF versus SST.

FIG. 5. Relationship between cloud radiative forcings and SST in the entire tropics. (a) LW CRF versus SST. (b) SW CRF versus SST.

FIG. 6. Anomalies of LW CRF (W m^{-2}) averaged from January to August. (a) 1987. (b) 1998.

FIG. 7. Distributions of LW CRF (W m^{-2}) averaged from January to August. (a) Mean of 1985, 1986 and 1989. (b) 1987. (c) 1998.

FIG. 8. Pressure-longitude cross section of zonal wind (ms^{-1}) averaged from $5^{o}S$ to $5^{o}N$ from January to August. (a) Mean of 1985, 1986 and 1989. (b) 1987. (c) 1998.

FIG. 9. Distribution of sea level pressure (mb). (a) Mean of 1985, 1986 and 1989. (b) 1987. (c) 1998.

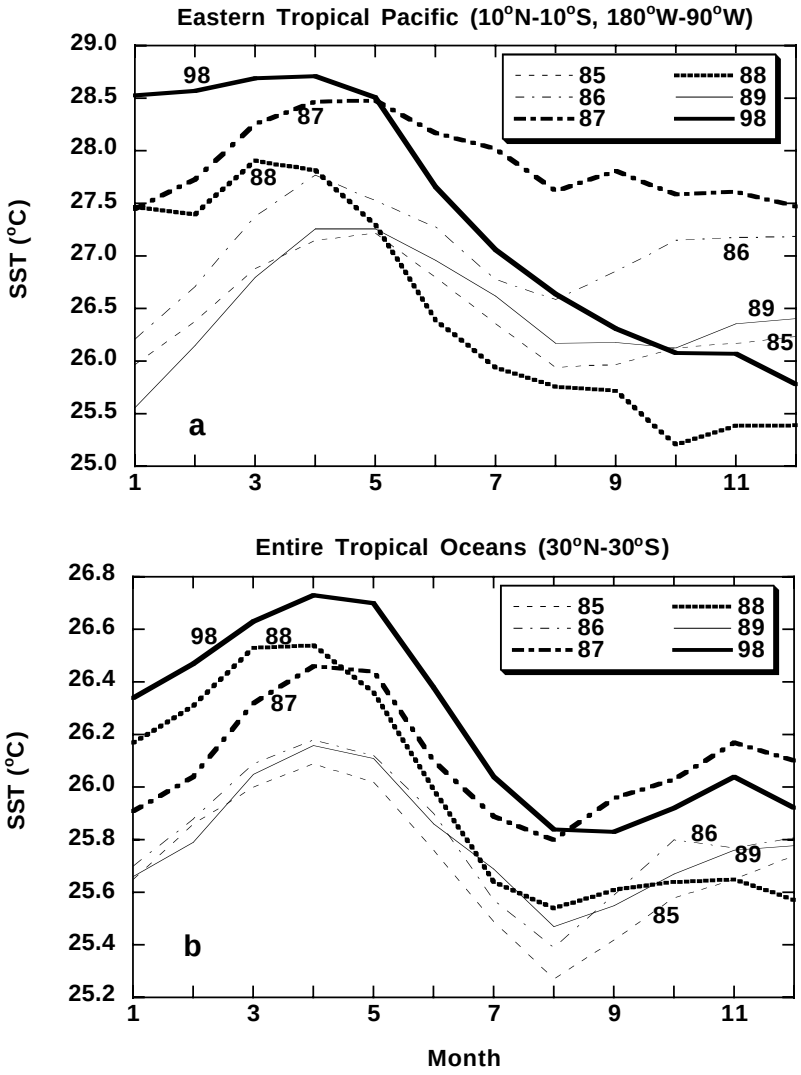
Eastern Tropical Pacific (10°N-10°S, 180°W-90°W)
SST (°C)
29.0
28.5
28.0
27.5
27.0
26.5
26.0
25.5
25.0
1
3
5
7
9
11
85
86
87
88
89
98
a
Entire Tropical Oceans (30°N-30°S)
SST (°C)
26.8
26.6
26.4
26.2
26.0
25.8
25.6
25.4
25.2
b
Month

Figure 1

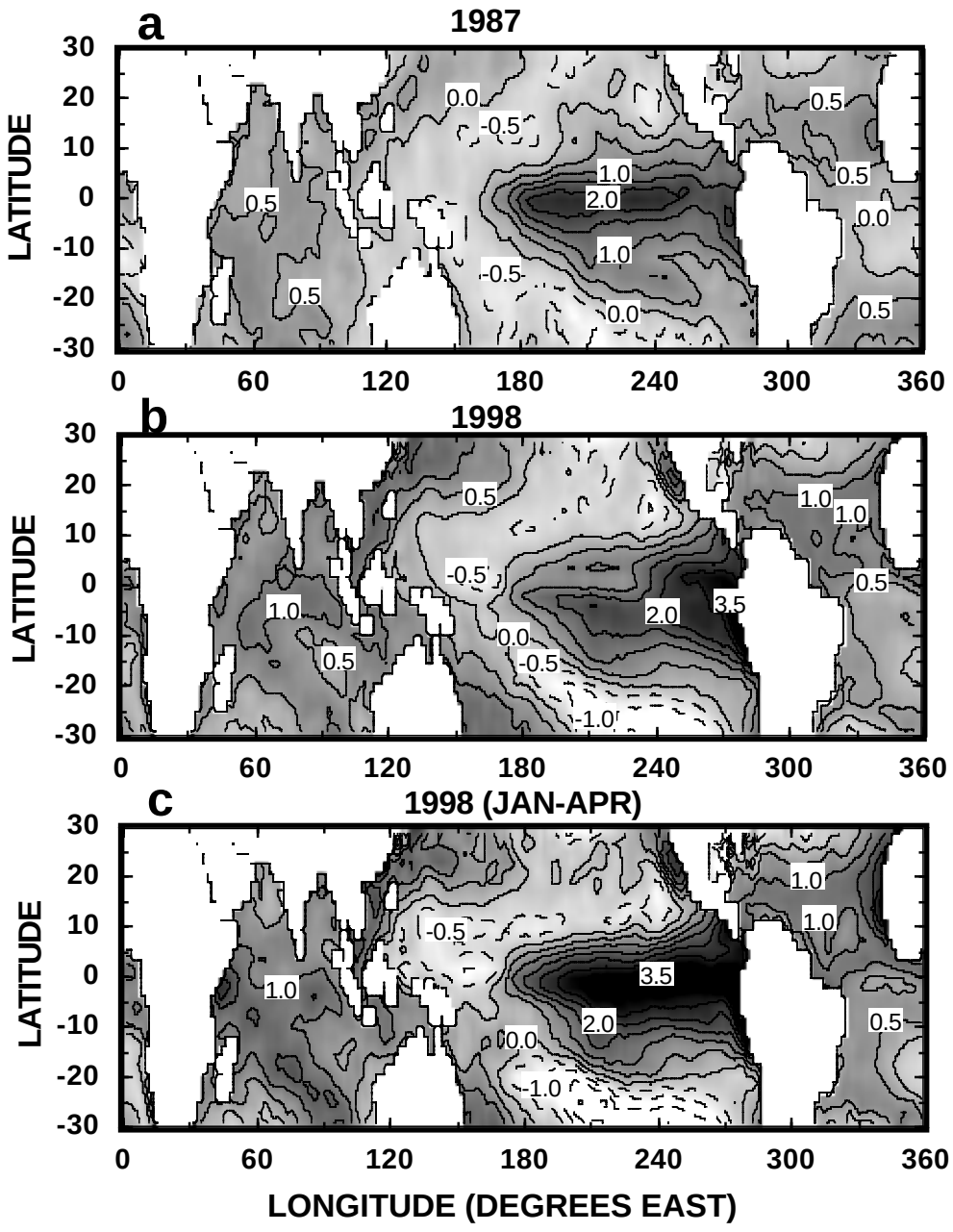
a
1987
b
1998
c
1998 (JAN-APR)
LATITUDE
LONGITUDE (DEGREES EAST)
30
20
10
0
-10
-20
-30
0
60
120
180
240
300
360
0.0
-0.5
0.5
1.0
2.0
3.5
-1.0

Figure 2

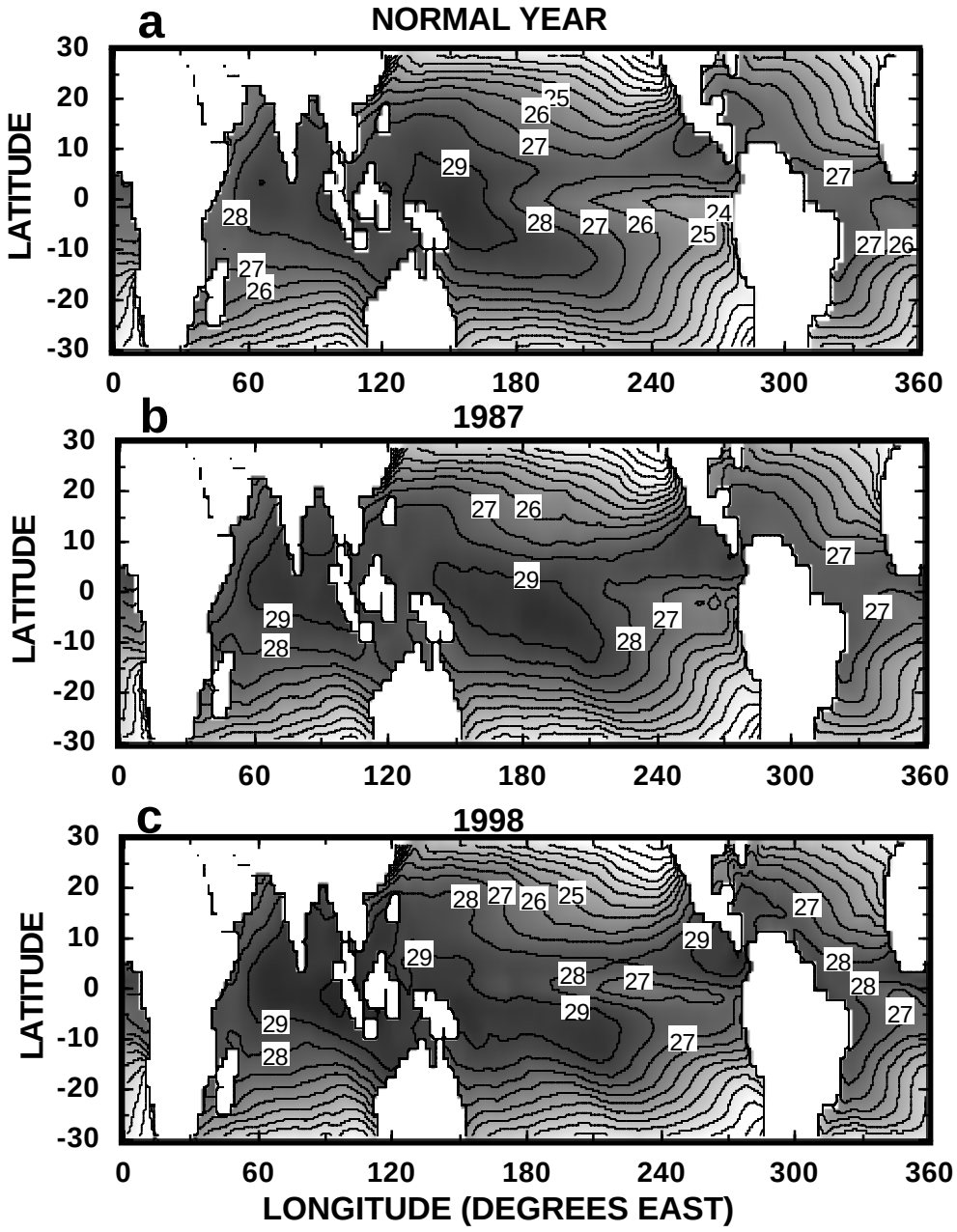
a
NORMAL YEAR
b
1987
c
1998
LATITUDE
LONGITUDE (DEGREES EAST)
30
20
10
0
-10
-20
-30
0
60
120
180
240
300
360

Figure 3

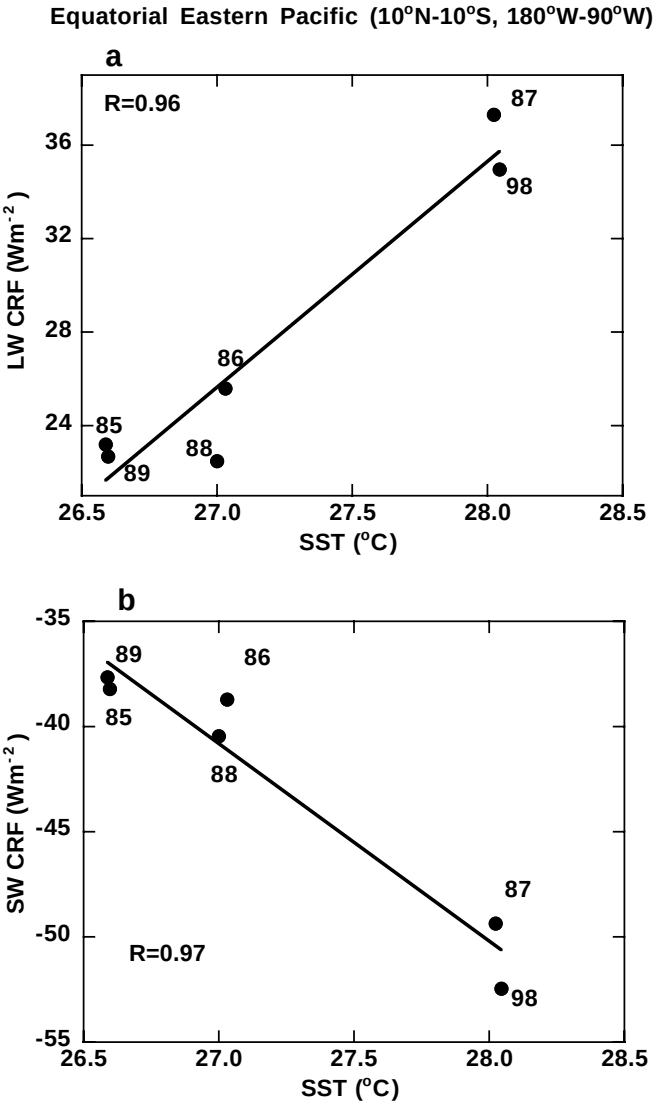
Equatorial Eastern Pacific (10°N-10°S, 180°W-90°W)
a
R=0.96
87
98
86
85
88
89
LW CRF (Wm-2)
SST (°C)
b
R=0.97
SW CRF (Wm-2)
SST (°C)

Figure 4

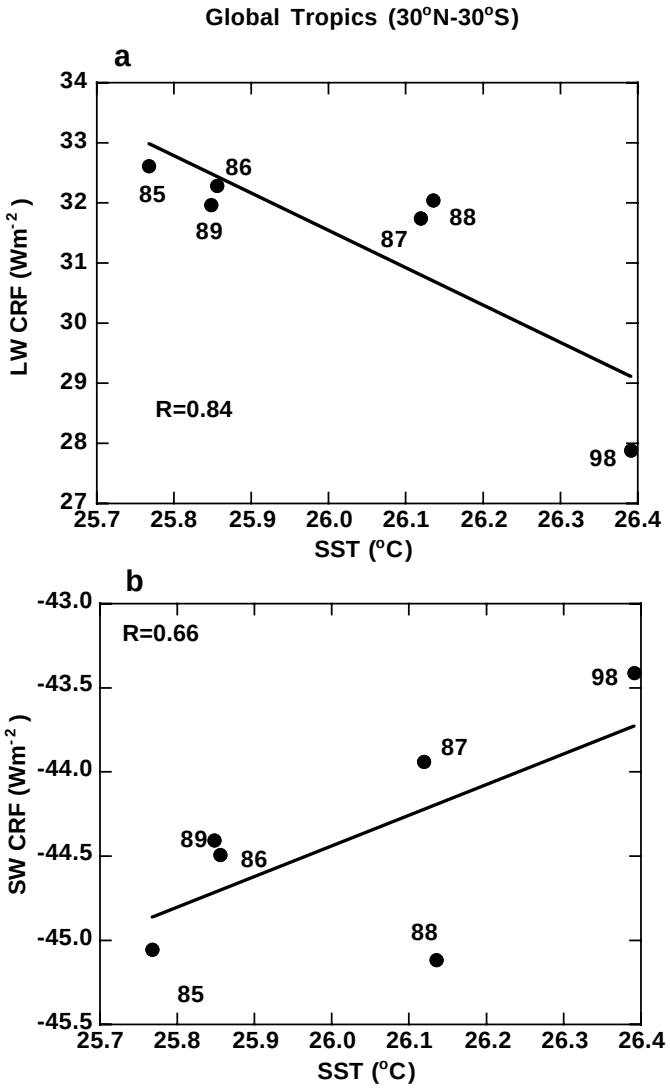
Global Tropics (30°N-30°S)
a
LW CRF (Wm-2)
SST (°C)
R=0.84
85
86
89
87
88
98
b
SW CRF (Wm-2)
SST (°C)
R=0.66
98
87
89
86
88
85

Figure 5

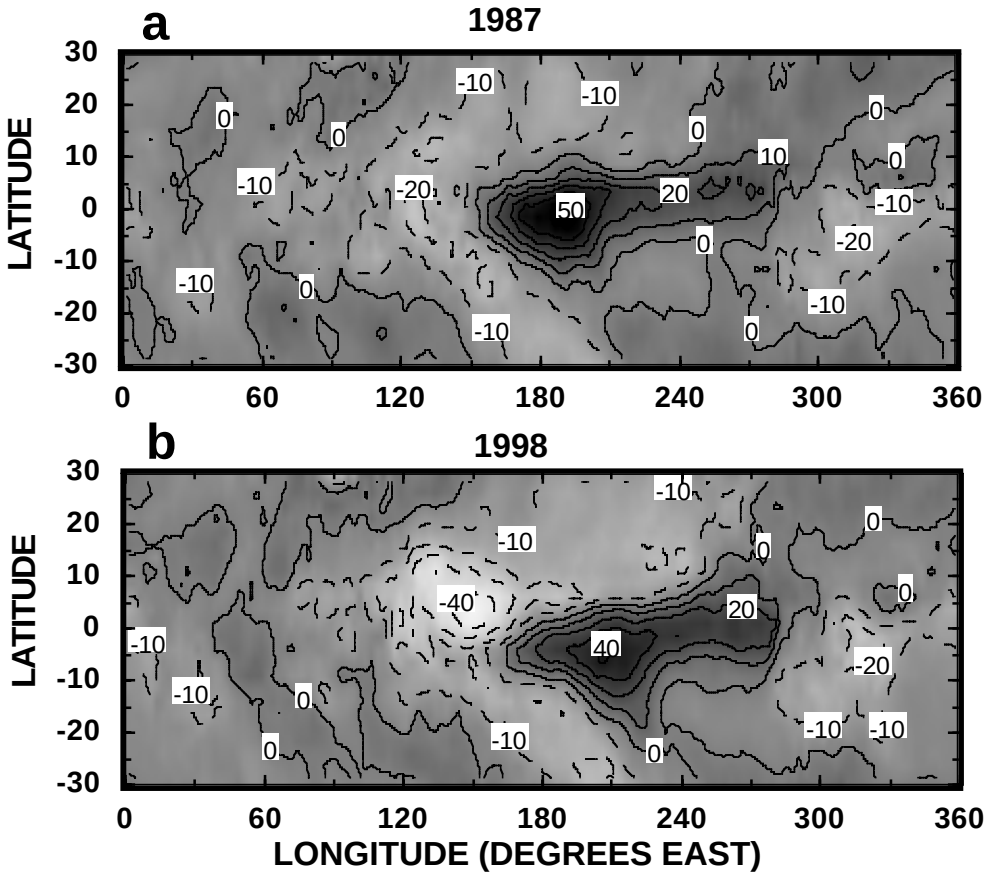
a
1987
b
1998
LATITUDE
LONGITUDE (DEGREES EAST)
30
20
10
0
-10
-20
-30
0
60
120
180
240
300
360
-10
-10
0
0
0
0
10
0
-10
-10
-20
20
50
0
-20
-10
-10
0
-10
0
-10
0
0
-10
-40
20
0
-10
40
-20
-10
0
-10
-10
0
-10
0

Figure 6

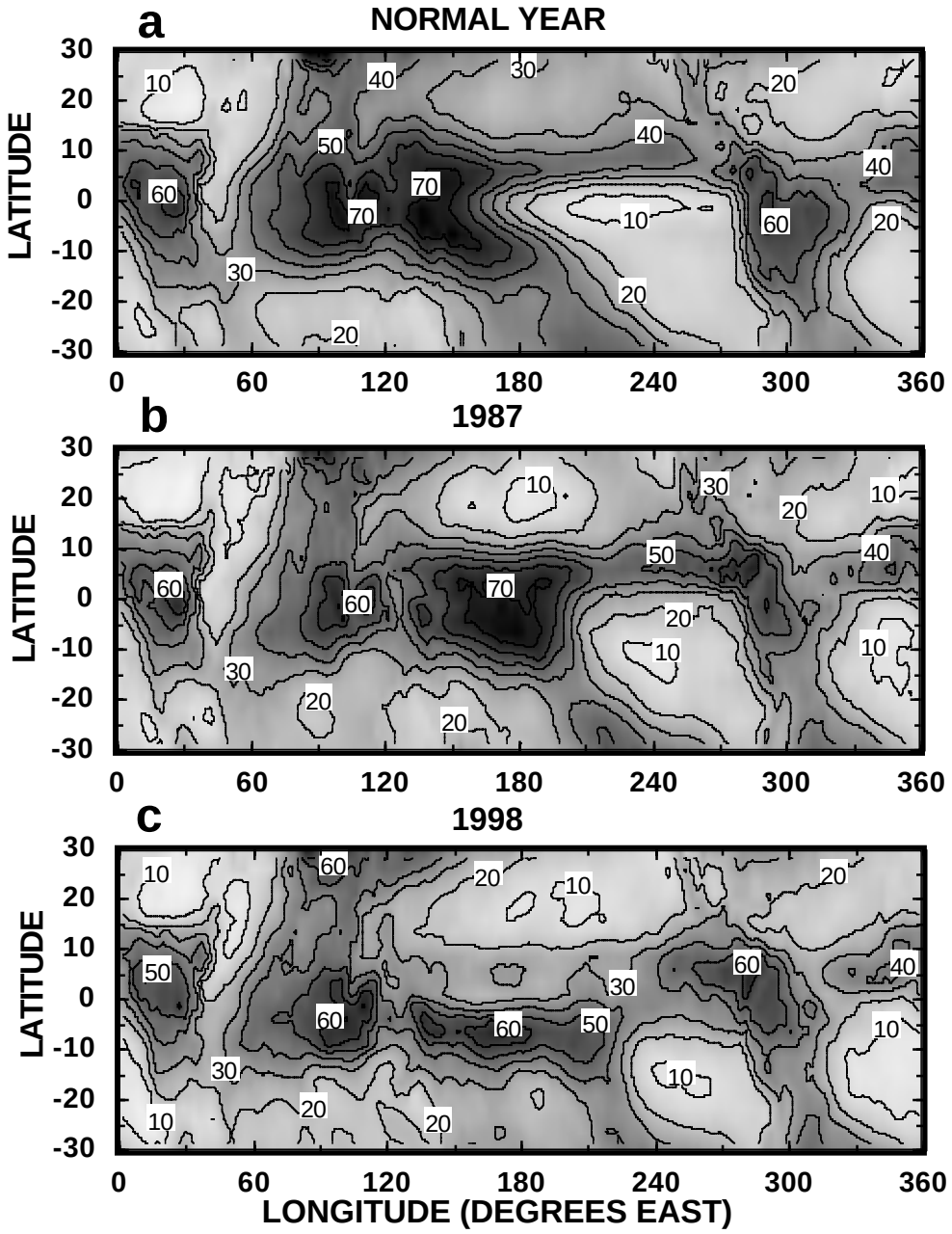
a
NORMAL YEAR
b
1987
c
1998
LATITUDE
LONGITUDE (DEGREES EAST)
30
20
10
0
-10
-20
-30
0
60
120
180
240
300
360

Figure 7

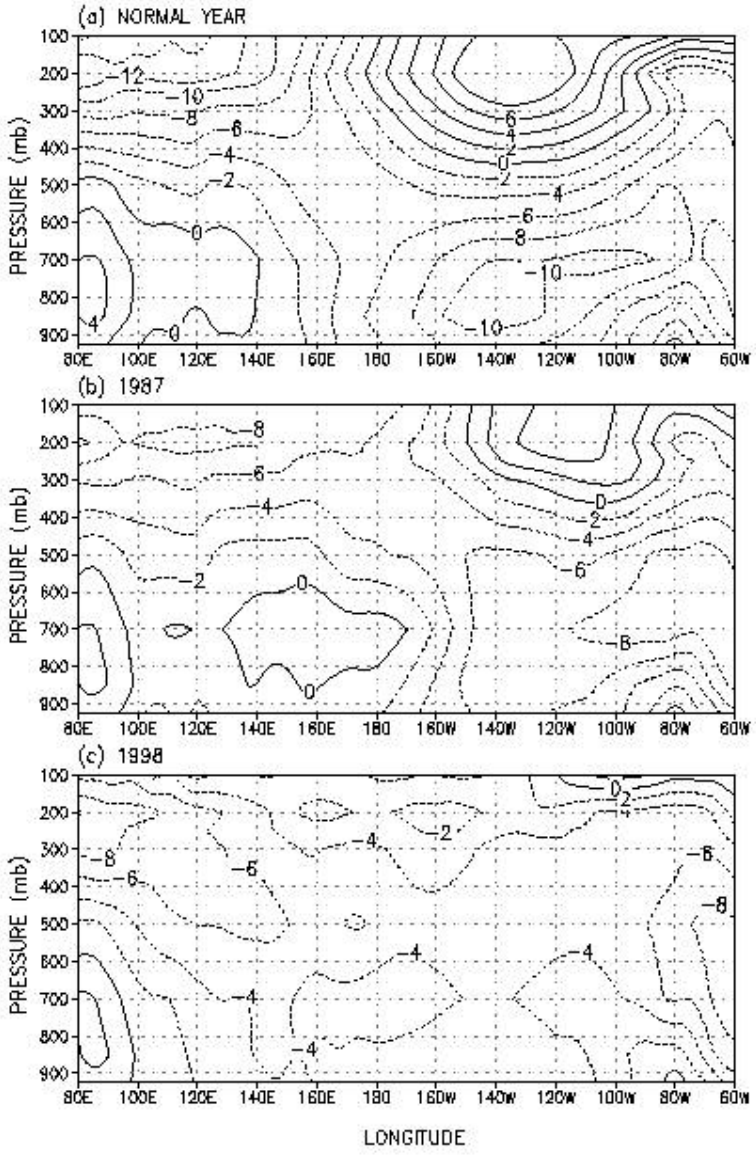
(a) NORMAL YEAR
(b) 1987
(c) 1998
PRESSURE (mb)
LONGITUDE
80E
100E
120E
140E
160E
180
160W
140W
120W
100W
80W
60W

FIGURE 8

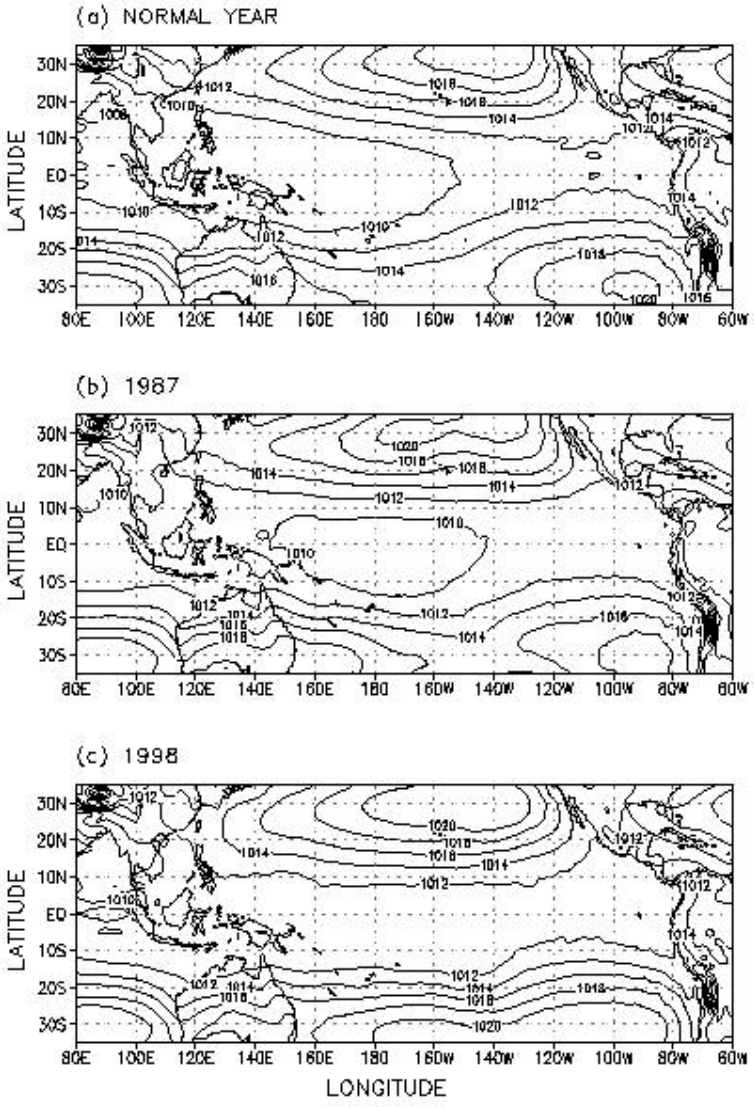
(a) NORMAL YEAR
(b) 1987
(c) 1998
LATITUDE
LONGITUDE
30N
20N
10N
EQ
10S
20S
30S
80E
100E
120E
140E
160E
180
160W
140W
120W
100W
80W
60W

FIGURE 9